Identification and immuno-electron microscopy localization of p40, a protein component of immunosuppressive virus-like particles from *Leptopilina heterotoma*

Hsiling Chiu[†], **Jorge Morales**[†], and **Shubha Govind**
Department of Biology and the Graduate Center, City College of The City University of New York, 138th Street and Convent Avenue, New York, NY 10031, USA

Abstract

Lamellocytes are specialized larval blood cells of *Drosophila* that carry out encapsulation of metazoan pathogens such as parasitoid wasps. Large virus-like particles (VLPs) from two closely related virulent parasitoid wasp species, *Leptopilina heterotoma* and *Leptopilina victoriae*, suppress the host encapsulation response by promoting lysis of lamellocytes. The molecular basis of VLP–lamellocyte interaction and lamellocyte lysis is not understood. Here, it was shown that mature VLPs are composed of at least four major proteins. Polyclonal antisera against the most abundant *L. heterotoma* VLP protein, p40, cross-reacted with the most abundant *L. victoriae* VLP protein, p47.5. Immuno-electron microscopy (EM) of the long gland–reservoir complex revealed that p40 was expressed early in VLP biogenesis and was detected along with VLP precursors within the long gland cells and lumen. In the reservoir, VLPs had an angular core, resembled mature particles and p40 was detected outside the VLP cores. Immuno-EM staining of mature VLPs from both species localized the p40 and p47.5 proteins largely to the periphery of the VLPs and along the VLP spike-like projections. p40 staining was observed in VLP-treated host haemocytes. *In vitro*, anti-p40 antibody almost completely blocked the ability of *L. heterotoma* VLPs to promote lamellocyte lysis. Anti-p40 antibody blocked lysis by *L. victoriae* VLPs by >50 %. It is proposed that the VLP surface proteins p40 and p47.5 share antigenic determinants and significantly contribute to the strong virulence of their Hymenopteran hosts.

INTRODUCTION

In nature, *Drosophila* serves as the host for a number of different microbial commensals, pathogens, pests and parasites (Ashburner, 1989). When strains of parasitoid wasps introduce eggs into the haemocoel of non-permissive or resistant *Drosophila* larvae, a strong and specific innate immune response of encapsulation is observed. This encapsulation reaction is characterized by the proliferation and differentiation of haematopoietic precursors in the lymph gland and the appearance of immune effector cells that quickly surround the wasp egg within many cell layers (Russo *et al*., 1996; Lanot *et al*., 2001; Sorrentino *et al*., 2002). The immune effector cells in the *Drosophila* haemolymph are plasmatocytes, lamellocytes and crystal cells, collectively referred to as haemocytes (Rizki & Rizki, 1984a; Carton & Nappi, 1997). Plasmatocytes are primarily phagocytic, but are also thought to be involved in recognition of the parasite egg. Lamellocytes are disc-shaped adhesive cells and form the bulk of the capsule. Crystal cells are thought to carry enzymes for melanization reactions and to participate in the

melanization of the capsule. Ultimately, encapsulation and melanization lead to death of the parasite (Vass & Nappi, 2000).

Parasitoid wasp eggs can, by a variety of mechanisms, often escape or evade this encapsulation, leading to their evolutionary success (Schmidt *et al*., 2001). *Leptopilina heterotoma* and *Leptopilina victoriae*, Cynipid wasp species, are sister species (Schilthuizen *et al*., 1998) and are both highly virulent. These wasps actively suppress the encapsulation reaction in their *Drosophila* hosts by two mechanisms: (i) infection by either wasp leads to the apoptotic depletion of haematopoietic precursors, although it is not known how the observed apoptosis is triggered (Chiu & Govind, 2002); (ii) wasp infection introduces virus-like particles (VLPs) into the host haemocoel that promote the lysis of mature lamellocytes (Rizki & Rizki, 1984b, 1990; Morales *et al*., 2005). VLP-induced lysis of lamellocytes does not appear to involve apoptosis (Chiu & Govind, 2002). These strategies of active immune suppression allow the wasp to inactivate and neutralize the cellular defence system of *Drosophila* and ensure optimal developmental opportunity for the wasp's progeny. The effect of VLPs appears to be specific and limited to haemocytes (Rizki & Rizki, 1990, 1994).

In *L. heterotoma* and *L. victoriae*, VLP precursors originate in cells of the long gland, an organ present in female wasps. Precursors undergo assembly within the long gland lumen and pass into the lumen of the reservoir via a connecting duct. In the reservoir lumen, VLPs undergo morphogenesis (Rizki & Rizki, 1984b; Morales *et al*., 2005). Several surface projections that have been referred to previously as spikes arise from the core (Rizki & Rizki, 1990; Morales *et al*., 2005). When incubated with intact *L. heterotoma* or *L. victoriae* VLPs *in vitro*, lamellocytes lose their typical discoidal appearance, as well as their ability to adhere. Instead, they become bipolar in shape and undergo degenerative changes, leaking cytoplasm at the elongated tips (Rizki & Rizki, 1990; Chiu & Govind, 2002). While VLPs of *L. heterotoma* and *L. victoriae* are similar in morphology and appear to act in a similar manner *in vitro*, we have recently found that *L. heterotoma* is more virulent than *L. victoriae* in both *in vivo* and *in vitro* assays (Morales *et al*., 2005). The molecular mechanisms by which VLPs promote lamellocyte lysis and the molecular basis for differences in virulence between *L. heterotoma* and *L. victoriae* are completely unknown. In this study, we have begun to analyse the molecular basis of host–parasite interactions by characterizing the basic constituents of VLP proteins. We report that the most abundant VLP proteins, p40 of *L. heterotoma* and p47.5 of *L. victoriae*, share antigenic determinants and play an important role in promoting the lysis of lamellocytes. Based on immuno-electron microscopy (EM) observations of *L. heterotoma*, we have shown that p40 is expressed early in VLP biogenesis and is associated with VLP precursors throughout VLP biogenesis and assembly. p40 became localized to the VLP surface during VLP morphogenesis in the reservoir. Both p40 and p47.5 were localized to the surface and spikes of mature VLPs. Finally, anti-p40 antibody made against *L. heterotoma* VLPs inhibited the ability of VLPs from both *L. heterotoma* and *L. victoriae* to promote lamellocyte lysis, suggesting that VLPs from both wasp species share antigenic determinants that contribute to virulence of the parasitoids.

METHODS

Insect stocks

L. heterotoma and *L. victoriae* were grown on *Canton S* and *ry506* strains of *Drosophila melanogaster*. Haemocytes from *D. melanogaster* strain *yellow vermilion hopscotchTum-l/Basc (y v hopTum-l/Basc;* Hanratty & Dearolf, 1993) were used to evaluate the *in vitro* effect of VLPs on haemocytes.

Antibody production, protein analysis and immuno-detection of p40

VLP-containing fluid was extracted from glands and reservoirs dissected in PBS; untreated fluid was used for VLP purification on a Nycodenz gradient (Rizki & Rizki, 1984b, 1990). Ultraviolet absorbance at 280 nm and the Bradford method (Bradford, 1976) were used to quantify proteins. A purified VLP preparation from *L. heterotoma* was used as an antigen to inject mice. Injections and bleeding (polyclonal serum) were performed at the Antibody Facility of Princeton University. Proteins in VLPs and fluid were processed for SDS-PAGE on a 9 %, 0·75 mm thick, acrylamide minigel, according to standard protocols (Laemmli, 1970; Sambrook *et al*., 1989). Proteins were either stained with silver stain (Bio-Rad) or transferred to nitrocellulose membranes. Membranes were probed with the anti-p40 antibody (diluted 1: 1000, 1 h at room temperature), followed by treatment with alkaline phosphatase-linked secondary antibody (Sigma). For cell-staining experiments, haemocytes from *y v hop^Tum-l^/Basc* were incubated with purified VLPs (or with untreated fluid) for 2–4 h, the medium was removed and cells were air dried for 30 min. Cells were fixed (2 % formaldehyde), washed (PBS with 1 % Triton X-100), blocked (wash solution with 2 % BSA, 1 h) and probed with primary anti-p40 antibodies (diluted 1: 1000) that were visualized by an FITC-labelled secondary goat anti-mouse IgG (Immunotech). A Zeiss Axioplan compound fluorescent or Bio-Rad confocal microscope was used for imaging stained cells.

EM

To determine whether VLPs are associated with the wasp egg, *Drosophila* larvae were dissected 20–30 min after infection and samples of wasp eggs were collected and prepared for scanning EM (SEM) as described by Morales (2005). To study VLP–lamellocyte interactions, haemocytes from *hop^Tum-l^/Y* larvae were incubated with *L. heterotoma* VLP fluid *in vitro* for 30 min and samples were processed for microscopy. To analyse the distribution of p40 in wasp tissues and mature VLPs, the long gland–reservoir complex and purified VLP pellets were fixed in glutaraldehyde, formaldehyde and picric acid and embedded in LR White resin, as described by Newman *et al*. (1982). Thin sections were treated with primary anti-p40 antibody (diluted 1: 30, 30 min, room temperature) and stained with goat anti-mouse secondary antibodies linked to 6 nm gold beads (Aurion; diluted 1: 10, 30 min, room temperature). A Zeiss transmission electron microscope (EM902) and a Zeiss scanning electron microscope (DSM940) were used to visualize samples. High-resolution SEM images were captured with a Hitachi S4700.

Inhibition of bipolar cell formation by primary antibody

VLP-containing fluid containing 30 μg protein in 10 μl PBS dissected from *L. heterotoma* or *L. victoriae* glands was treated with the primary antibody or non-immune mouse serum. The amount of protein in the antibody sera from immune and non-immune mice ranged from 70 to 80 μg μl^{-1}. These mixtures were gently agitated for 30 min at room temperature. Haemocytes obtained from 10 *hop^Tum-l^/Y* animals were pooled in 210 μl 10 % fetal bovine serum in PBS, separated into seven equal portions and treated as follows at 25 °C: portions 1 and 2 were treated with either *L. heterotoma* or *L. victoriae* fluid (positive controls, no antibody); portions 3 and 4 with 5 μl anti-p40 antibody-treated fluid from either of the wasps (experimental, immune); portions 5 and 6 with non-immune mouse serum-treated fluid; portion 7 with PBS (negative control, non-immune). In order to obtain a high fraction (>80 %) of bipolar lamellocytes and allow comparison of equivalent VLP activities, blood cells were incubated with *L. victoriae* fluid for 8 h and with *L. heterotoma* fluid for 4–5 h. The number of bipolar cells formed was counted using a Nikon inverted microscope. Standard error and *z* tests for independent proportions were performed as described by Dawson & Trapp (2004).

RESULTS

VLPs in *L. heterotoma* are synthesized in the long gland and are thought to be stored in the reservoir (Rizki & Rizki, 1984a; Fig. 1a and b). A series of large, peripheral secretory cells (Fig. 1b, arrows) surround an internal, narrow concentric lumen (Fig. 1a and b, labelled L). In between the lumen and the secretory cells, a layer of small endothelial-like cells (intimal layer) is clearly seen (Fig. 1a and b, arrowheads). At the distal end, the lumen expands into a sac-like structure referred to as the 'nose' (Fig. 1a–c, labelled N).

SEM studies

In transmission EM (TEM) studies, it has been reported that *L. heterotoma* and *L victoriae* VLP spikes sometimes terminate in larger knob-like structures (Rizki & Rizki, 1994; Morales *et al*., 2005). To determine whether this was the case and to examine the surface structure of mature VLPs, we prepared VLP samples for SEM. These preparations confirmed the general organization and variability observed in TEM analysis of VLP morphology (Rizki & Rizki, 1994). At lower magnification by SEM, VLPs from the long gland–reservoir complex appeared in small groups or strung together (Fig. 2a). In such preparations, VLPs appeared to adhere to each other via the ends of their spikes. These spike ends (knobs) were enlarged relative to the mean width of the spikes. However, in contrast to TEM images where only some spikes seemed to terminate in knobs, SEM images revealed the presence of knobs on all spikes (see Fig. 2c). This apparent difference in morphology could be due to differences in fixation or in preparation of materials in SEM and TEM methods.

To determine whether VLPs were associated with the wasp egg soon after oviposition, we dissected newly infected wild-type host larvae and fixed eggs for observations by SEM. We found that a few VLPs were indeed present on the egg surface (Fig. 2b and c). In several cases, we found a clear association of the VLP spike with the egg surface (e.g. Fig. 2c, white arrowhead). Both single particles (Fig. 2c) and compound particles (not shown) were associated with wasp eggs.

To examine VLP–lamellocyte binding, we incubated purified VLPs with lamellocytes from *hop^Tum-l* mutant larvae *in vitro*. Thirty minutes after this incubation, VLP-treated haemocyte samples were fixed and processed for SEM. In these preparations, we found clusters of VLPs adhering to the lamellocyte membrane. VLPs in these clusters appeared to adhere to the lamellocyte membrane via spikes/knobs (Fig. 2d and e). Together, these results suggested that VLP spikes and possibly the knobs have an adhesive function and may harbour molecules involved in VLP–haemocyte interactions.

VLP proteins

To estimate the number and size of proteins that make up the VLPs, gradient-purified VLPs from *L. heterotoma* and *L. victoriae* were separated by SDS-PAGE and visualized by silver staining (Fig. 3a, lanes 1 and 2). Silver staining is 10–50 times more sensitive than Coomassie brilliant blue protein staining and can visualize as little as 0·1 ng protein mm^{-2} (Merril *et al*., 1981). Four major protein bands (with apparent molecular masses of 87·5, 75, 72·5 and 40 kDa) were observed in VLPs of *L. heterotoma*. There were at least eight major proteins in the *L. victoriae* VLP preparation (Fig. 3a, lane 2, arrowhead, stars and dots). Several proteins present at lower abundance are also observed in both VLP preparations (Fig. 3a, lanes 1 and 2, dots). The most abundant *L. heterotoma* VLP protein was 40 kDa, whereas in *L. victoriae* it was roughly 47·5 kDa (Fig. 3a, lanes 1 and 2, arrows). Since VLPs are synthesized and stored in the long gland and reservoirs, respectively, we also examined the protein composition of the fluid obtained from these organs by silver staining. All of the major VLP proteins observed in Fig. 3(a, lanes 1 and 2) also appear to be represented in the untreated fluid prepared from

dissected long glands and reservoirs (Fig. 3a, lanes 3 and 4), although their relative proportions were different. As expected, the number of proteins in the untreated fluid was higher.

Mouse polyclonal antibodies against purified intact *L. heterotoma* particles reacted specifically with the predominant p40 protein of *L. heterotoma* VLP (called anti-p40 antibody hereafter; Fig. 3b, lanes 1 and 2). This anti-p40 antibody also cross-reacted with p47.5 of *L. victoriae* VLPs (Fig. 3c). This observation suggested that these predominant VLP components have common antigenic determinants.

Expression of p40 in wasp tissues

To determine whether p40 protein is expressed during the early stages of VLP biogenesis in the long gland and to examine how p40 distribution is modified as VLPs undergo maturation, we first dissected the long gland–reservoir complex and stained it with anti-p40 antibody. While the main body of the long gland showed clear and intense staining, the 'nose' of the long gland did not stain (Fig. 1c). In addition, staining of the reservoir was much less intense than that of the long gland (Fig. 1c). Other organs of the female wasp (such as ovaries) and even host tissues (e.g. larval fat body) remained completely unstained (not shown).

To examine the distribution of p40 protein at higher resolution, we performed immuno-EM on thin sections through the long gland 'nose' (Fig. 1d, position A), the main body of the long gland (Fig. 1d, positions B and C) and the reservoir (Fig. 1d, position D) (the orientation of positions A–D are indicated in Fig. 1d). p40 protein was visualized by secondary antibodies linked to gold beads. In negative controls where primary antibody was not included in the staining protocol, background levels of adherent gold beads were virtually absent (Fig. 4, panels a4, b4 and b8; Fig. 5, panels c2, c9 and d4; Fig. 6d).

The 'nose' of the long gland (Fig. 1d, position A) is an expanded region of the lumen, surrounded only by small endothelial-like cells. The nose contains many small vesicle-like structures, but lacks electron-dense particles resembling immature VLPs. Consistent with the whole-mount staining result (Fig. 1c), immuno-gold staining showed very low or undetectable levels of p40 in this region (Fig. 4; compare panels a1–a3 with a4). However, within secretory cells located around position B of the long gland (see Fig. 1d for orientation), the level of p40 protein was very high (Fig. 4; compare panels b1–b3 with a1–a3; panel b4 represents the negative control). Furthermore, p40 was clearly associated with VLP precursors (electron-dense structures found within canals and the long gland lumen; also see Morales *et al.*, 2005) being secreted into the rough canals (surrounded by membranous projections; see Fig. 4, panel b3; arrows point to clusters, whereas membranous projections are apparent in panel b4). As mentioned above, these canals connect the secretory cells to the lumen. At the same location, but within the lumen adjacent to the secretory cells (position B, lumen is wide), we found a very high level of p40 protein assembled on to electron-dense clusters of immature VLPs (Fig. 4 compare b5–b7 with b8). Significantly, vesicle-like structures present in the 'nose' were not present in the lumen of position B, even though this region is continuous with the 'nose'.

At a more proximal position, where the lumen tapered into the body of the long gland, (Fig. 1d, position C), we found clusters of immature VLP precursors in the secretory cell canals and lumen, and, as described above, strong anti-p40 staining. Anti-p40 binding was especially strong around the VLPs present within the smooth canal lumen (Fig. 5, panel c1) and the long gland lumen (Fig. 5, panels c6–c8). Immature particles in the lumen at position C (Fig. 5, panels c6–c10) were morphologically slightly more complex than particles in the lumen at position B (Fig. 4, panels b5–b8). Some particles at position C appeared to have spikes (arrows), had acentric electron-light regions (arrowheads) and resembled the particles described by Rizki & Rizki (1984b). Morphologically, these particles were intermediate in complexity between the simpler precursors found in the secretory cells and the mature particles found in the reservoir.

To examine VLP morphology and p40 staining in the reservoir, sections were prepared from position D (Fig. 5, panels d1–d4). VLPs in this region appeared to be more differentiated and morphologically had begun to resemble mature VLPs. Individual VLPs appeared to be continuous with one another, separated by electron-light 'tracks' (Fig. 5, panels d2 and d3, arrows). These 'tracks' merged with the electron-light matrix surrounding the VLPs. The number of gold particles that bound to sections prepared from the reservoir was not as high as that observed in the long gland sections, an observation that was consistent with the whole-mount staining result (Fig. 1c). However, gold particles were clearly present above background levels (Fig. 5; compare panels d2 and d3 with d4) and localized the p40 protein mostly to the immediate vicinity of the maturing particles. Whilst in the reservoir, it is possible that p40 is not as accessible to the anti-p40 antibody as it is in the long gland, resulting in a lowered signal in both whole-mount and immuno-EM experiments. The composition of the electron-light matrix surrounding the VLPs in the reservoir is not known.

p40 and p47.5 localize to the VLP surface and spikes

To confirm that the p40 and p47.5 proteins are part of mature VLPs and to determine their distribution on the VLPs, we performed immuno-EM on sections of gradient-purified VLPs isolated from female wasp reservoirs and counted the number of gold beads present on the VLP surface and inside each VLP. We found that while some p40 and p47.5 protein was localized within the VLPs, most was distributed on the surface of the VLPs (Fig. 6a–d). The number of gold beads per VLP present on the VLP surface was significantly higher ($P<0.001$) than that within the VLP core (Fig. 6e) for both *L. heterotoma* (15·9/20; *n*=22) and *L. victoriae* (9·9/11·1; *n*=22). Furthermore, each VLP had four to six spikes and roughly 20 % of the secondary antibody-linked gold bead signal was associated with the spikes. Because this 'peripheral' anti-p40 signal accounted for the majority of the total anti-p40 antibody binding, we concluded that p40 and p47.5 proteins are primarily located on the surface and spikes of the VLPs.

p40 and p47.5 in Drosophila haemocytes

Because p40 protein is present on mature VLPs, and mature VLPs interact with lamellocytes or are internalized by plasmatocytes (Rizki & Rizki, 1994), we expected p40 to be present in association with both cell types. To test this idea, we probed *hop^{Tum-l}* larval haemocytes with *L. heterotoma* or *L. victoriae* fluid and with anti-p40 antibody. Lamellocytes exposed to VLPs from either species become bipolar in shape before undergoing lysis (Fig. 7a, c and e, arrows). When these fluid-treated lamellocytes were incubated sequentially with primary anti-p40 antibody and FITC-linked secondary antibody, immuno-reactivity to the p40 and p47.5 proteins was clearly observed (Fig. 7d and f). As expected, there was no binding of antibody to PBS-treated lamellocytes and these lamellocytes retained their discoidal shape throughout the incubation period (Fig. 7a and b). When a confocal microscope was used to visualize p40 protein, antibody-binding signal was present within *L. heterotoma* fluid-treated plasmatocytes (Fig. 7g and h). In this experiment, the fluorescent signal from lamellocytes was not as strong, possibly because lamellocytes are extremely thin and flat or because p40 protein remained on the lamellocyte surface.

A common function for p40 and p47.5

Having established that p40 and p47.5 proteins are associated with VLPs when they interact with host haemocytes, we tested whether p40 and p47.5 proteins play a role in immune suppression. We examined whether the anti-p40 antibody could interfere with VLP-induced cell lysis. Anti-p40 antibody was added to long gland–reservoir fluid prior to its addition to haemocytes. We allowed for differences in the activity levels of the *L. heterotoma* and *L. victoriae* VLPs by imposing conditions such that VLP samples exhibited similar activity (i.e.

~85 % of lamellocytes became bipolar). We found that anti-p40 antibody strongly reduced the percentage of lamellocytes that become bipolar (Fig. 7i). Only 7 % of lamellocytes become bipolar in response to *L. heterotoma* VLPs in the presence of the antibody, compared with control experiments in which over 85 % of lamellocytes assumed bipolar morphology (Fig. 7i). Consistent with its cross-reactivity, anti-p40 significantly reduced the percentage of lamellocytes made bipolar by *L. victoriae* VLPs (from 87·3 and 82·8 % in control experiments to 45·8 %), although this effect was weaker than that observed with *L. heterotoma* VLPs (Fig. 7i). These results directly link VLP proteins from both wasp species to the lysis of *Drosophila* lamellocytes. Because they are involved functionally in promoting morphological changes in lamellocytes, these proteins may play a direct role either in the initial recognition of lamellocytes or, at a subsequent step, in altering lamellocyte cell-surface properties or lamellocyte shape changes. The observation that anti-p40 antibody blocked bipolar cell formation *in vitro* is thus consistent with the idea that the VLP surface proteins p40 and p47.5 are somehow involved in VLP–lamellocyte interactions.

DISCUSSION

In recent years, remarkable progress has been made in our understanding of the processes and mechanisms governing the innate immune responses of *Drosophila* (reviewed by Bodian *et al.*, 2004; Brennan & Anderson, 2004). Infectious parasitoid wasps inactivate the cellular immune response of encapsulation by depositing proteinaceous VLPs along with the egg. In this study, we have presented a first description of the biochemical constituents of the highly immune-suppressive *L. heterotoma* and *L. victoriae* VLPs that subvert the cellular immune responses of *D. melanogaster*. Additionally, immuno-EM analysis of VLP biogenesis within the *L. heterotoma* long gland–reservoir complex revealed two distinct steps in VLP biogenesis (in the long gland) and morphogenesis (in the reservoir) that have been unreported previously: (i) in the long gland lumen, *L. heterotoma* VLP precursors appear to increase in size, progressing through different stages of differentiation (VLPs with electron-light cores and peripheral spikes; Fig. 5, panels c6–c10); (ii) in the reservoir, *L. heterotoma* VLPs are present either singly or in arrays and are surrounded by a lipid bilayer. VLP cores are intersected with bilayers that divide the particles into segments. Mature, gradient-isolated particles have a pentagonal/hexagonal core, with multiple spikes. In these respects, *L. heterotoma* VLPs resemble VLPs of *L. victoriae* (Morales *et al.*, 2005).

Not all species of the genus *Leptopilina* produce VLPs with spikes. In *Leptopilina boulardi*, the only other species from which VLPs have been reported, spikes are absent (Dupas *et al.*, 1996), but VLPs are believed to carry out the same biological function, i.e. modify lamellocyte morphology and interfere with encapsulation (Labrosse *et al.*, 2003). The presence of spikes in VLPs from both *L. heterotoma* and *L. victoriae* (but not in VLPs from *L. boulardi*) thus constitutes a clear morphological parameter for VLP classification. Scanning electron micrographs of VLPs show that VLP spikes enlarge into structures that we refer to as 'knobs'. However, knobs are not observed frequently in transmission electron micrographs (Rizki & Rizki, 1990, 1994; Morales *et al.*, 2005). Scanning electron micrographs of freshly deposited wasp eggs (from the host haemocoel) confirm that VLPs are associated with the eggs and suggest that the association may be mediated by VLP spikes/knobs. Furthermore, SEM studies of VLPs incubated with lamellocytes confirm VLP interaction with their target cells via spikes and knobs. Together, these observations suggest that spikes on the VLPs may play an adhesive role or may mediate recognition and/or contact between VLPs and wasp eggs and between VLPs and lamellocytes. Understanding the nature of these interactions is clearly of great importance, as they represent the interface between host and parasite.

Expression of p40 in *L. heterotoma*

To address the mechanism by which VLPs interact with host lamellocytes, we characterized purified *L. heterotoma* and *L. victoriae* VLPs and consistently observed strong protein bands of 40 and 47·5 kDa. Staining studies showed that p40 expression was restricted to the tissues where VLPs originate and develop. p40 expression was not detected in wasp ovaries or in extracts prepared from male wasps (data not shown).

Immuno-staining experiments revealed that, within the long gland, p40 was not detected in the 'nose' of the long gland, but was expressed within canals of secretory cells proximal to the 'nose'. The expression of p40 was coincident with the site at which electron-dense VLP precursors were first seen and its presence was continuously observed during stages of VLP biogenesis and morphogenesis, although staining intensity was much higher in the long gland (during VLP biogenesis), compared with in the reservoir (during VLP maturation). The reason for this difference is not known. Nevertheless, immuno-EM from both positions revealed that the presence of p40 was not restricted to the electron-dense cores of the maturing VLPs. Instead, gold beads were also observed within the matrix surrounding the VLP cores and spikes. This localization of p40 in the vicinity of developing VLPs is consistent with the final presence of p40 on the surface and spikes of mature VLPs. The presence of intact VLPs within plasmatocytes and lamellocytes has been observed by EM after their incubation with VLPs (Rizki & Rizki, 1994), and it was therefore not surprising that we can identify the presence of p40 (or p47.5) protein in these cells after treatment with VLPs from *L. heterotoma* or *L. victoriae* (Fig. 7). Thus, anti-p40 antibody can be used as a means of tracking the presence of VLPs in the wasp as well as in the host.

Functional conservation of p40 and p47.5

VLPs from both *L. victoriae* and *L. heterotoma* are made up of several proteins. However, when mice were injected with intact *L. heterotoma* VLPs, we were surprised initially to find that the polyclonal serum developed by two mice cross-reacted specifically with the most abundant protein, p40. In retrospect, this can be explained by the fact that p40, as an abundant surface protein, was the primary antigen detected by the mouse immune system. The cross-reactivity of *L. heterotoma* anti-p40 with p47.5 from *L. victoriae* on the Western blot, as well as surface localization of p47.5 on mature *L. victoriae* VLPs, argues for structural, and possibly functional, conservation between the most abundant proteins of each VLP. Interestingly, in ELISA or Western blot analyses, we found that anti-p40 antibody showed no detectable cross-reactivity with proteins within crude lysate prepared from glands of *L. boulardi* (unpublished results). It is worth noting that, unlike *L. heterotoma/L. victoriae* VLPs that induce lamellocyte lysis, *L. boulardi* VLPs do not induce lamellocytes to become bipolar and lyse. These observations suggest that *L. boulardi* VLPs not only lack spikes, but may also lack the surface protein associated with the spikes of *L. heterotoma/L. victoriae* VLPs. While further molecular characterization of VLP proteins in these three species is necessary to confirm this prediction, it appears that the *L. heterotoma/L. victoriae* VLPs form a synapomorphy for the two taxa, serving as phylogenetically informative characters for this clade.

Further evidence for functional conservation of p40 and p47.5 comes from results of antibody inhibition experiments, where we found that not only do the anti-p40 antibodies almost completely inhibit the effect of *L. heterotoma* VLPs to promote bipolar cell formation, but that they also have the same effect on *L. victoriae* VLPs. We therefore propose that the p40 and p47.5 proteins are structurally and functionally related and contribute to the high degree of virulence conferred by the VLPs. An alternative interpretation of the antibody-inhibition experiments is that the anti-p40 antibodies cause VLPs to cluster, masking lamellocyte-binding sites and thereby preventing VLPs from acting on lamellocytes. The molecular function and mode of action of p40 and p47.5 are currently unknown. Because these proteins appear to be

localized to the VLP spikes and surface, one possibility is that VLPs are a vehicle for p40/ p47.5 delivery and that p40/p47.5 is directly involved in lamellocyte lysis. In an alternative scenario, the two abundant proteins may provide a structure to the VLPs themselves and mediate VLP–lamellocyte interactions. We are in the process of characterizing the molecular structures of p40 and p47.5, with the goal of shedding light on their molecular functions and providing insight into the role of VLP proteins in lamellocyte lysis and immune suppression.

Acknowledgments

References

Ashburner, M. A Laboratory Handbook. Cold Spring Harbor, NY: Cold Spring Harbor Laboratory; 1989. Drosophila.

Bodian DL, Leung S, Chiu H, Govind S. Cytokines in *Drosophila* hematopoiesis and cellular immunity. Prog Mol Subcell Biol 2004;34:27–46. [PubMed: 14979663]

Bradford MM. A rapid and sensitive method for the quantitation of microgram quantities of protein utilizing the principle of protein-dye binding. Anal Biochem 1976;72:248–254. [PubMed: 942051]

Brennan CA, Anderson KV. *Drosophila:* the genetics of innate immune recognition and response. Annu Rev Immunol 2004;22:457–483. [PubMed: 15032585]

Carton Y, Nappi AJ. *Drosophila* cellular immunity against parasitoids. Parasitol Today 1997;13:218–227. [PubMed: 15275074]

Chiu H, Govind S. Natural infection of *D. melanogaster* by virulent parasitic wasps induces apoptotic depletion of hematopoietic precursors. Cell Death Differ 2002;9:1379–1381. [PubMed: 12478476]

Dawson, B.; Trapp, RG. Basic and Clinical Biostatistics. Vol. 4. New York: McGraw Hill; 2004.

Dupas S, Brehelin M, Frey F, Carton Y. Immune suppressive virus-like particles in a *Drosophila* parasitoid: significance of their intraspecific morphological variations. Parasitology 1996;113:207–212. [PubMed: 8811846]

Hanratty WP, Dearolf CR. The *Drosophila Tumorous-lethal* hematopoietic oncogene is a dominant mutation in the *hopscotch* locus. Mol Gen Genet 1993;238:33–37. [PubMed: 8479437]

Labrosse C, Carton Y, Dubuffet A, Drezen JM, Poirie M. Active suppression of *D. melanogaster* immune response by long gland products of the parasitic wasp *Leptopilina boulardi*. J Insect Physiol 2003;49:513–522. [PubMed: 12770630]

Laemmli UK. Cleavage of structural proteins during the assembly of the head of bacteriophage T4. Nature 1970;227:680–685. [PubMed: 5432063]

Lanot R, Zachary D, Holder F, Meister M. Postembryonic hematopoiesis in *Drosophila*. Dev Biol 2001;230:243–257. [PubMed: 11161576]

Merril CR, Goldman D, Sedman SA, Ebert MH. Ultrasensitive stain for proteins in polyacrylamide gels shows regional variation in cerebrospinal fluid proteins. Science 1981;211:1437–1438. [PubMed: 6162199]

Morales, J. PhD thesis. The City University of New York; USA: 2005. Immune suppression by parasitoid wasps of Drosophila: studies on virus-like particles, virulence, and genome-wide expression analysis.

Morales J, Chiu H, Oo T, Plaza R, Hoskins S, Govind S. Biogenesis, structure, and immune suppressive effects of virus-like particles of a *Drosophila* parasitoid, *Leptopilina victoriae*. J Insect Physiol 2005;51:181–195. [PubMed: 15749103]

Newman GR, Jasani B, Williams ED. The preservation of ultrastructure and antigenicity. J Microsc 1982;127:RP5–RP6.

Rizki, TM.; Rizki, RM. The cellular defense system of *Drosophila melanogaster*. In: King, RC.; Akai, H., editors. Insect Ultrastructure. Vol. 2. New York: Plenum; 1984a. p. 579-604.

Rizki RM, Rizki TM. Selective destruction of a host blood cell type by a parasitoid wasp. Proc Natl Acad Sci U S A 1984b;81:6154–6158. [PubMed: 6435126]

Rizki RM, Rizki TM. Parasitoid virus-like particles destroy *Drosophila* cellular immunity. Proc Natl Acad Sci U S A 1990;87:8388–8392. [PubMed: 2122461]

Rizki TM, Rizki RM. Parasitoid-induced cellular immune deficiency in *Drosophila*. Ann N Y Acad Sci 1994;712:178–194. [PubMed: 7910721]

Russo J, Dupas S, Frey F, Carton Y, Brehelin M. Insect immunity: early events in the encapsulation process of parasitoid *(Leptopilina boulardi)* eggs in resistant and susceptible strains of *Drosophila*. Parasitology 1996;112:135–142. [PubMed: 8587797]

Sambrook, J.; Fritsch, EF.; Maniatis, T. Molecular Cloning: a Laboratory Manual. Cold Spring Harbor, NY: Cold Spring Harbor Laboratory; 1989.

Schilthuizen M, Nordlander G, Stouthamer R, van Alphen JJM. Morphological and molecular phylogenetics in the genus *Leptopilina (Hymenoptera: Cynipoidea: Eucoilidae)*. Syst Entomol 1998;23:253–264.

Schmidt O, Theopold U, Strand M. Innate immunity and its evasion and suppression by hymenopteran endoparasitoids. Bioessays 2001;23:344–351. [PubMed: 11268040]

Sorrentino RP, Carton Y, Govind S. Cellular immune response to parasite infection in the *Drosophila* lymph gland is developmentally regulated. Dev Biol 2002;243:65–80. [PubMed: 11846478]

Vass E, Nappi AJ. Developmental and immunological aspects of *Drosophila*–parasitoid relationships. J Parasitol 2000;86:1259–1270. [PubMed: 11191902]
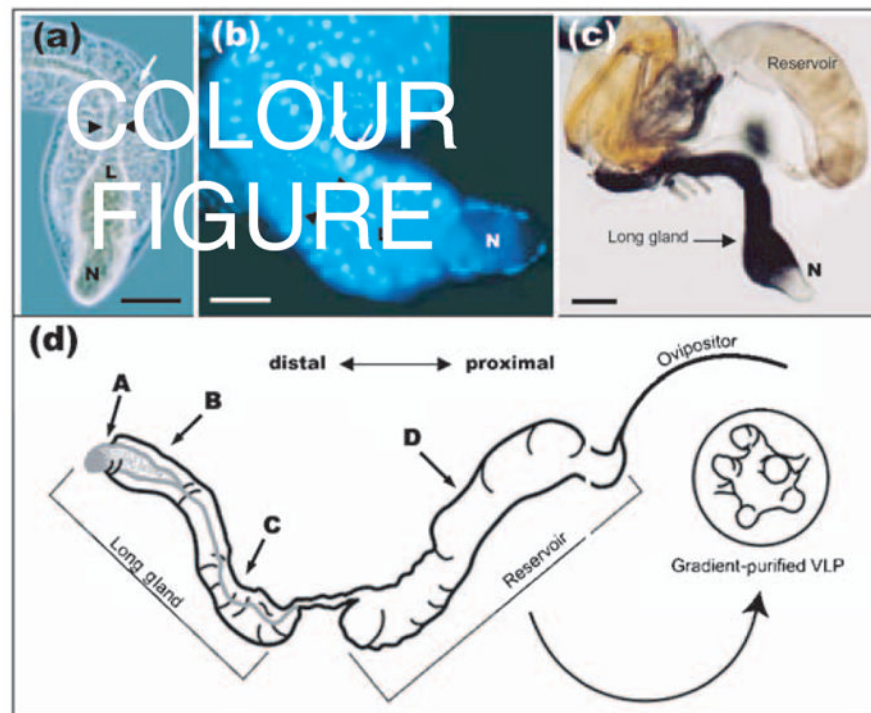
Fig. 1.
(a, b) Phase-contrast (a) and Hoechst-stained (b) micrographs showing the morphology of the *L. heterotoma* long gland. Arrows point to secretory cells and arrowheads to the lumen (L). Note that the lumen expands into the 'nose' (N) and is surrounded by a thin layer of smaller cells known as the intimal layer. Bars, 100 μm. (c) Indirect immuno-detection of p40 protein in the long gland–reservoir complex of *L. heterotoma* using anti-p40 antibody. Anti-p40 antibody (70 ng ml^{-1}) was detected by a secondary antibody linked to alkaline phospha-tase (diluted 1: 1000; Promega), giving a purple reaction product. The long gland shows strong staining, whilst the reservoir shows weaker staining. Bar, 200 μm. (d) Schematic representation of the long gland–reservoir complex indicating the positions from where sections were prepared for immuno-EM in Figs 4 and 5.
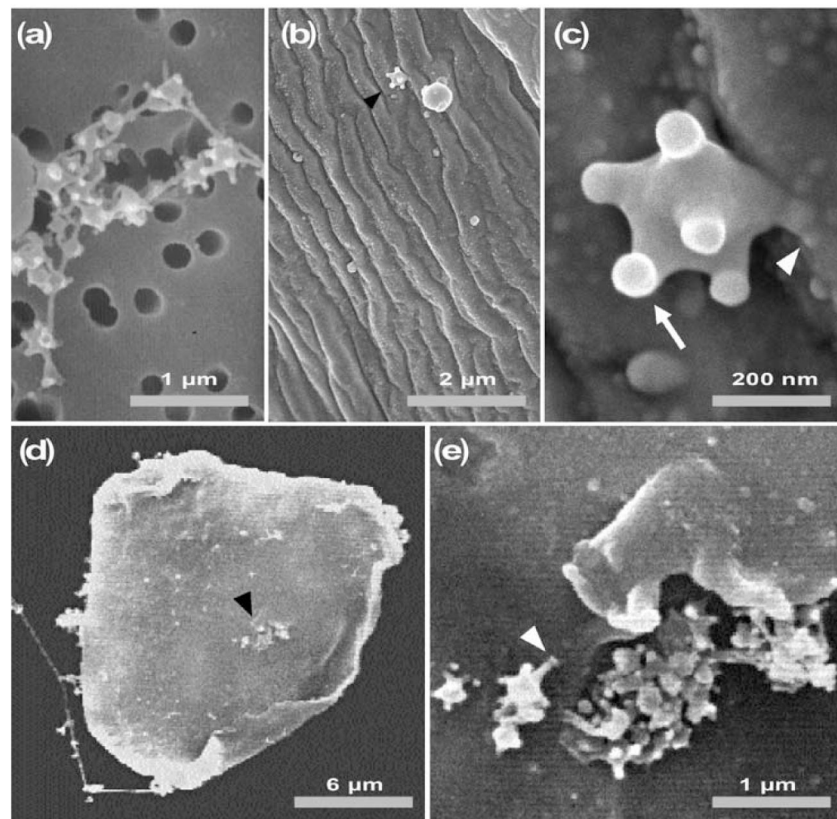
Fig. 2.
Scanning electron micrographs of *L. heterotoma* VLPs. (a) In untreated fluid, VLPs remain connected to one another. (b, c) VLPs on the surface of a wasp egg, 10–15 min after wasp infection. (d, e) Binding of VLPs to a lamellocyte after 30 min incubation. The arrowhead in (d) shows a cluster of VLPs; this area is enlarged in (e). The white arrowheads in (c) and (e) show the spike/knob structure of a VLP in contact with the surface of a wasp egg (c) and the surface of a lamellocyte (e), respectively. The arrowheads in (b) and (d) point to areas enlarged in (c) and (e), respectively.
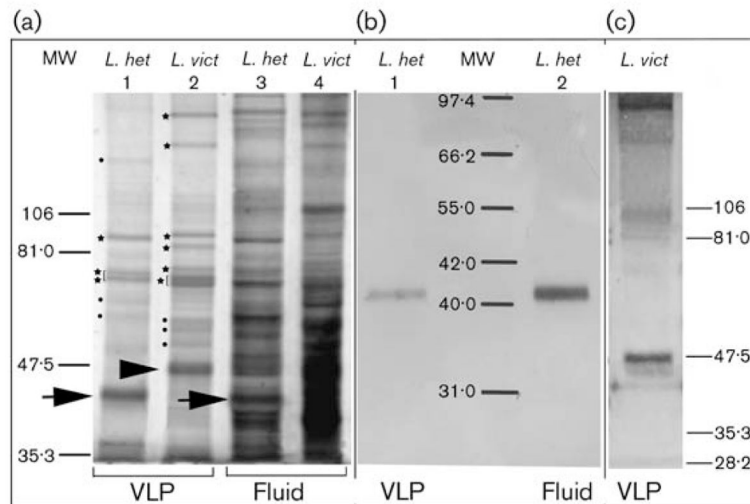
Fig. 3.
(a) Silver-stained SDS-polyacrylamide gel of *L. heterotoma* and *L. victoriae* VLP proteins. Stars and dots along lanes 1 and 2 indicate major and minor protein bands, respectively, that were observed reproducibly. Arrows indicate the *L. heterotoma* p40 protein, whereas the arrowhead points to the *L. victoriae* p47.5 protein. Lanes 1 and 2 were loaded with 2·1 μg protein and lanes 3 and 4 with 12 μg protein. (b, c) Western blot analysis using anti-p40 antibody. Lanes 1 and 2 in (b) contained 1·0 μg *L. heterotoma* VLP or fluid proteins, respectively. The lane in (c) contained 8 μg *L. victoriae* VLP proteins. The blot was overstained with substrates of alkaline phosphatase.
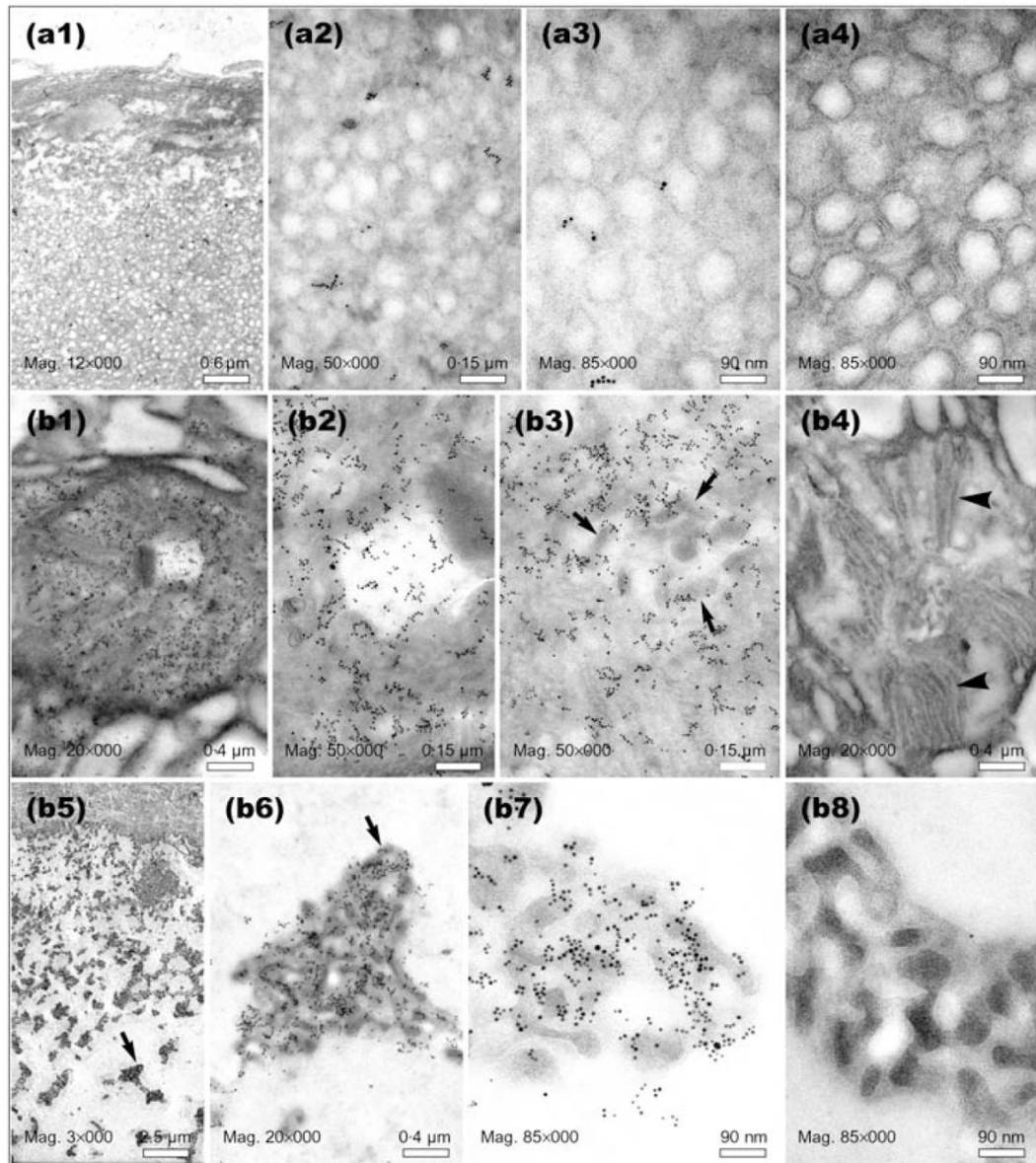
Fig. 4.
Immuno-EM of thin sections prepared from positions A and B of the *L. heterotoma* long gland (see Fig. 1d for orientation). Panels a1–a4 show preparations derived from the 'nose', panels b1–b4 through the 'rough' canals within secretory cells and b5–b8 through the lumen of the long gland. Panels a4, b4 and b8 are negative controls (no primary antibody). Arrows in panels b3, b5 and b6 point to clusters of immature VLPs. Arrowheads in panel b4 point to membranous projections found around the 'rough' canals into which immature VLPs are first secreted. Similar structures were found in secretory cells in the long gland at position C (see Fig. 5, panel c3, black arrowhead).
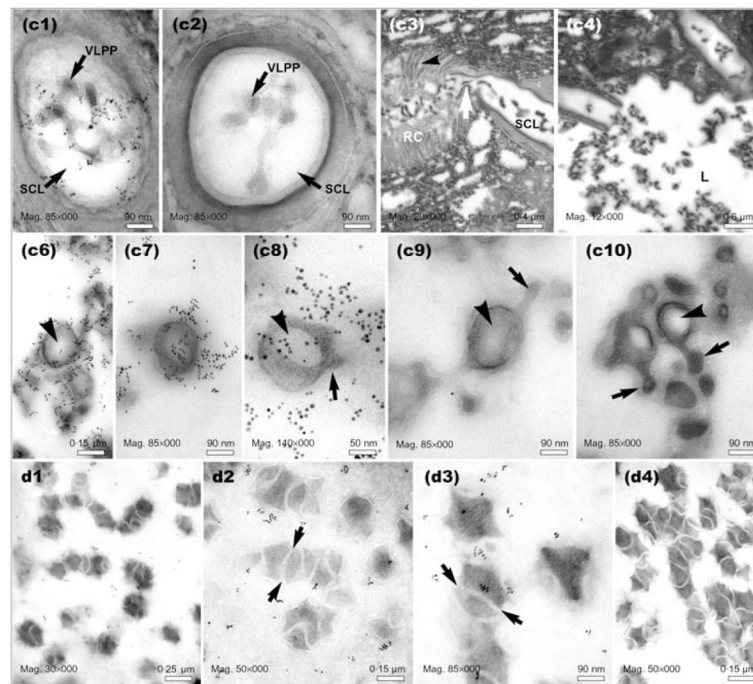
Fig. 5.
Electron micrographs of sections prepared from positions C and D of the *L. heterotoma* long gland and reservoir, respectively, as indicated in Fig. 1(d). Panels c1 and c2 show precursors of VLPs within the smooth canals (transverse sections). Smooth canals (SC) appear to be connected directly to rough canals (RC) (see white arrow in panel c3). The smooth canal empties into the long gland lumen (L) (panel c4). Panels c6–c10 show VLPs in the long gland lumen at position C. Some VLPs are spiked (arrows) and have acentric electron-light regions inside the VLP body (arrowheads). High levels of p40 are associated with developing VLPs (panels c6–c8). Panels d1–d4 show VLPs in the reservoir at position D (see Fig. 1d). Arrows show the presence of 'tracks' separating maturing VLPs. Panels c2, c9 and d4 are negative controls (primary antibody omitted), whereas samples in panels c3, c4 and c10 were not immuno-stained.
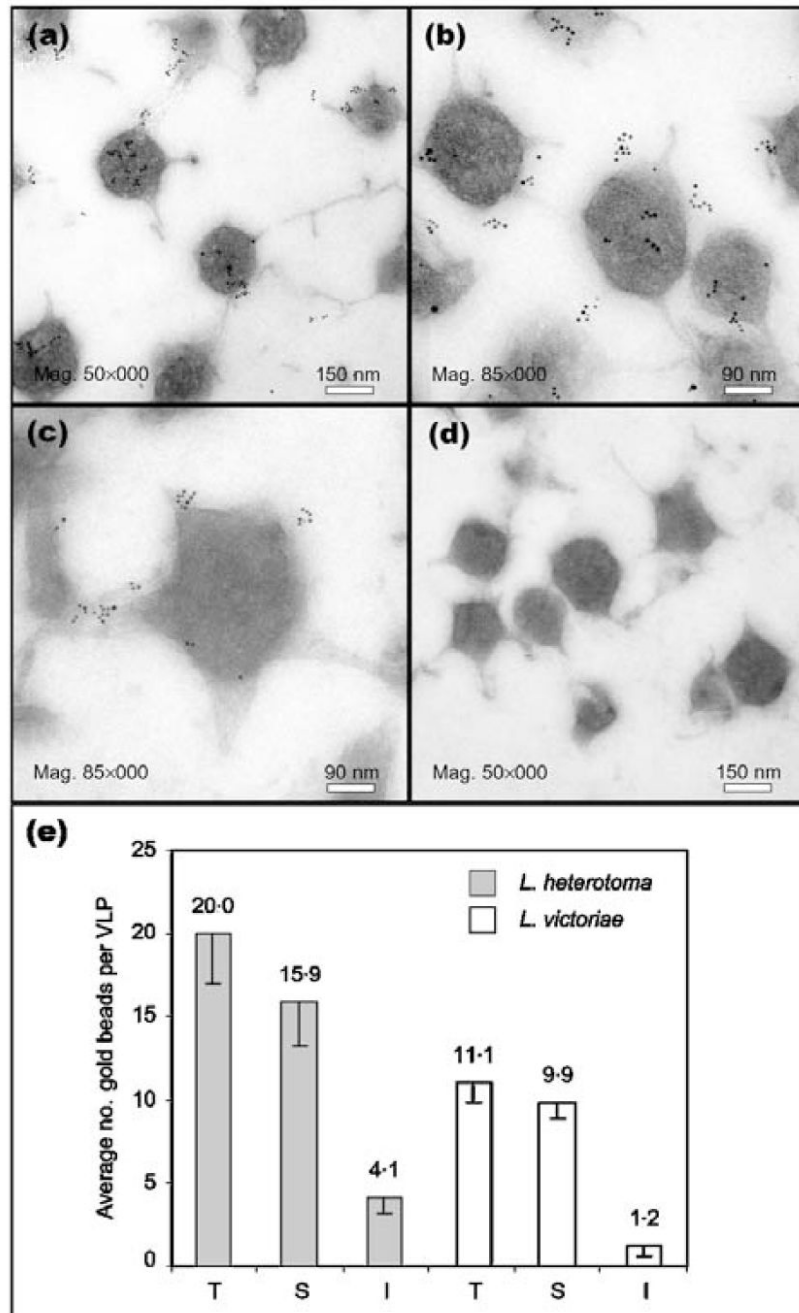
Fig. 6.
(a–d) Immuno-EM of gradient-purified VLPs. Localization of p40 protein on *L. heterotoma* VLPs (a, b) and p47.5 on *L. victoriae* VLPs (c). For the negative control (d), primary antibody was omitted. (e) Binding of primary antibody as measured by counting the number of gold beads adhering to the surface (S) or internal (I) regions of 22 VLPs from either wasp species. The sum of these two numbers is represented as the total (T) binding of gold beads to the VLPs.
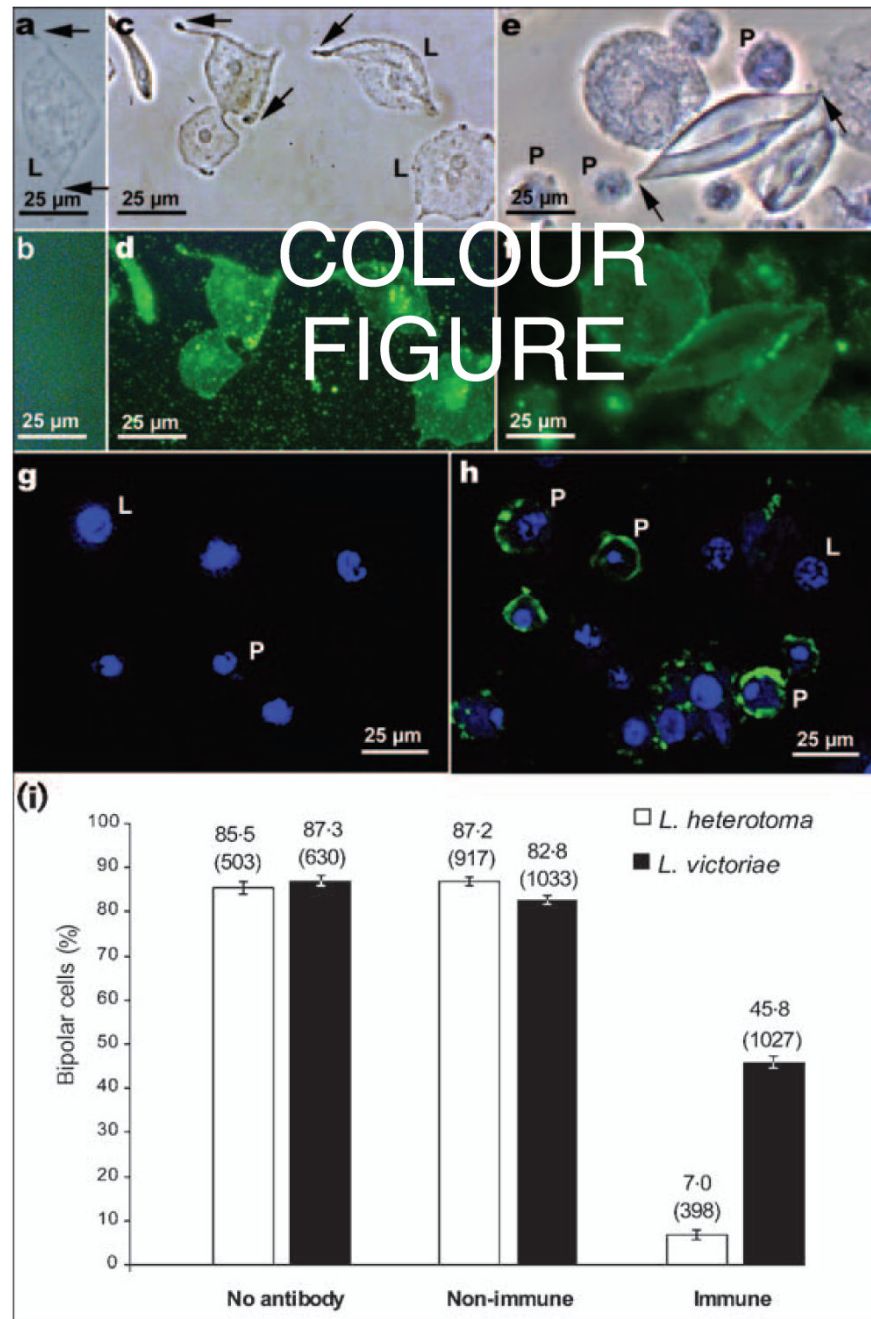
Fig. 7.
(a–h) Detection of p40 and p47.5 proteins by indirect immunofluorescence using anti-p40 antibodies. All haemocytes used were from hop^{Tum-l}/Y larvae and were treated with either *L. heterotoma* (a–d, g–h), or *L. victoriae* (e, f) fluid. For the negative controls (a, b), primary antibody was omitted. (a, c, e) Phase view of cells in (b), (d) and (f), where anti-p40 antibodies were visualized by FITC-linked secondary antibody. Arrows point to the tapering ends of the lamellocytes as they assume bipolar morphology prior to lysis. Untreated lamellocytes do not become bipolar (not shown). (g, h) Confocal images showing the association of hop^{Tum-l} haemocytes (counterstained with the nuclear dye TOTO-3) with anti-p40 antibody within plasmatocytes treated with *L. heterotoma* fluid (h) and the negative control (g). P,

Plasmatocyte; L, lamellocyte. (i) Inhibition of formation of bipolar cells by anti-p40 antibodies. The percentage of lamellocytes that became bipolar cells is noted on top of each bar. The total number of lamellocytes examined is indicated in parentheses. Non-immune: mouse serum was used as a negative control; immune: anti-p40 antibody-treated fluid from *L. heterotoma* or *L. victoriae*. Suppression of bipolar cell formation by the anti-p40 antibody was highly significant (*z*>16, *P*<0·003) in pairwise *z* tests for independent proportions between the no antibody/non-immune (negative controls) and the immune (experimental) *in vitro* assays with fluid from either wasp.